Barker, P.F., Camerlenghi, A., Acton, G.D., and Ramsay, A.T.S. (Eds.)
Proceedings of the Ocean Drilling Program, Scientific Results Volume 178

18. Data Report: Microfabric Analysis of Postglacial Sediments from Palmer Deep, Western Antarctic Peninsula[1]

Jennifer Pike,[2] Steven G. Moreton,[2,3] and Claire S. Allen[2]

ABSTRACT

The Antarctic Peninsula region is ideally suited to monitor how global change affects Antarctica because it is one of the most sensitive regions of the continent to rapid climate change. This has been clearly demonstrated by the recent break up of the Larsen A Ice Shelf. Drilling at Ocean Drilling Program Site 1098, Palmer Deep, western Antarctic Peninsula, recovered almost 50 m of sediments that record the paleoceanographic and paleoclimatic history of the region from the last glacial maximum through the rapid climate oscillations of deglaciation into the Holocene. This sedimentary section will provide a wealth of high-resolution paleoenvironmental data from Antarctica that will be useful for climate modelers and paleoceanographers alike. This data report presents the preliminary results of a high-resolution, microscale sediment fabric study of the postglacial sediments from Palmer Deep Site 1098. These sediments have previously been described as being annually laminated; however, this investigation shows that although the interpretation of this sequence as seasonal sediments is most likely correct, there are a number of features that indicate there is strong interannual variability affecting the laminations.

[1] Pike, J., Moreton, S.G., and Allen, C.S., 2001. Data report: Microfabric analysis of postglacial sediments from Palmer Deep, western Antarctic Peninsula. *In* Barker, P.F., Camerlenghi, A., Acton, G.D., and Ramsay, A.T.S. (Eds.), *Proc. ODP, Sci. Results,* 178, 1–17 [Online]. Available from World Wide Web: <http://www-odp.tamu.edu/publications/178_SR/VOLUME/CHAPTERS/SR178_18.PDF>. [Cited YYYY-MM-DD]
[2] Department of Earth Sciences, Cardiff University, PO Box 914, Cardiff CF10 3YE, United Kingdom.
pikej@cardiff.ac.uk
[3] NERC Radiocarbon Laboratory, Scottish Enterprise Technology Park, Rankine Avenue, East Kilbride G75 0QF, United Kingdom.

Initial receipt: 13 November 2000
Acceptance: 25 June 2001
Web publication: 5 November 2001
Ms 178SR-226

INTRODUCTION

The Antarctic Peninsula region of the Southern Ocean currently is the most rapidly warming region of Antarctica, with 2.5°C of warming documented for the last 50 yr (Jones et al., 1993; Leventer et al., 1996, and references therein). This climatic warming has been demonstrated in a dramatic way by the collapse of the Larsen A Ice Shelf (eastern Antarctic Peninsula) in January 1995 (Doake et al., 1998). Investigations of the west Antarctic fjord systems have demonstrated that understanding how sedimentary systems have responded to events of rapid climate change in the past is crucial to attempts to predict how this sensitive region will respond to current and future climate change (Domack et al., 1993; Domack and McClennen, 1996).

Palmer Deep is a series of three fault-bounded basins (Rebesco et al., 1998) situated on the inner continental shelf south of Anvers Island (Fig. F1) that act as a natural sediment trap in one of the most sensitive regions of the west Antarctic Peninsula in terms of oceanic conditions, sea ice dynamics, and, hence, biological productivity and climate (Domack et al., 1993; Domack and McClennen, 1996; Hofmann et al., 1996; Leventer, 1991; Leventer et al., 1996; Morris et al., 1998; Parkinson, 1998; Smith et al., 1999). During Ocean Drilling Program (ODP) Leg 178, a ~50-m-long core was recovered from 1012 m water depth in Palmer Deep Basin I (Site 1098) (Barker, Camerlenghi, Acton, et al., 1999). Near the base (43.34–46.34 meters composite depth) of the recovered sedimentary sequence is a ~3-m-thick interval of spectacularly laminated to thinly bedded orange-brown diatom ooze and blue-gray diatom-bearing terrigenous sediments (hereafter referred to as the "laminated unit") overlying a diamict containing prominent dropstones (Fig. F2). The laminated unit has been dated, using accelerator mass spectrometry (AMS) radiocarbon dating of acid-insoluble organic matter, to a calibrated age of 11.8–13.15 ka (Domack et al., 2001). The laminated unit comprises the first deposition following the retreat of the grounded ice sheet from Basin I (Rebesco et al., 1998) during the last deglaciation and, as such, sedimentation during a period of rapid and substantive climate change. The debate over whether this interval correlates with the time of the Antarctic Cold Reversal (Blunier et al., 1998) or is an expression of Northern Hemisphere warming during the Bølling/Allerød Interstadial that lags the Northern Hemisphere by 1500 yr will not be addressed here. However, it is interesting to note that in the more recent past, when most of the rest of west Antarctica was colder and windier during the Little Ice Age, the Antarctic Peninsula climate warmed (Leventer et al., 1993). The age of the diamict below the laminated unit is >13.15 ka (Domack et al., 2001), which is roughly in agreement with the uncalibrated radiocarbon age of ~11 ka given by Pudsey et al. (1994) for the retreat of the ice sheet across the western Antarctic Peninsula shelf.

The deglacial laminated unit has been ascribed an annual mechanism of formation (Leventer et al., 1998) consistent with present-day seasonality in the region. Sea ice coverage during the austral winter is associated with an impoverished flux of sedimentary particles (A. Leventer, pers. comm., 2001; unpublished sediment trap data). Spring heralds the onset of sea ice melting and water column stratification, which is associated with high biological primary productivity (e.g., Hofmann et al., 1996; Leventer, 1991) and flux to the seafloor. This is followed by the summer season of reduced primary productivity and

F1. Location of Palmer Deep, west Antarctic Peninsula, p. 9.

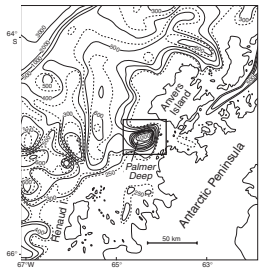

F2. Core photograph of Core 178-1098A-6H, p. 10.

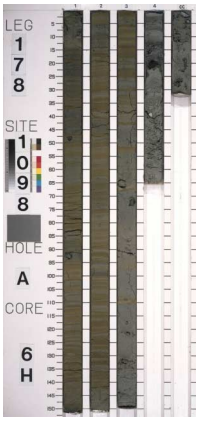

higher input of terrigenous sediments as ice-rafted debris (A. Leventer, pers. comm. 2001, unpublished sediment trap data). However, decadal- to centennial-scale climatic cycles have been recorded using biological proxies from the Antarctic Peninsula (Leventer et al., 1996) and other regions of the Southern Ocean (e.g., Leventer et al., 1993), and the radiocarbon age model for this laminated unit gives an annual sedimentation rate of 0.3 cm/yr (Domack et al., 2001). A significant amount of caution, therefore, should be applied when interpreting this postglacial laminated unit as being composed of annual sedimentary couplets, or varves.

The purpose of this data report is to present the preliminary results of a scanning electron microscope (SEM)-scale sediment fabric analysis of the postglacial laminated unit. An additional goal is to demonstrate the implications of lamina-scale sampling and the need for precise, high-resolution analysis of the phytoplankton assemblages preserved within the sediment layers before a firm annual mode of deposition can be ascribed.

MATERIALS AND METHODS

Thin Section Preparation and Analysis

The samples for this study were taken from ODP Core 178-1098A-6H (Barker, Camerlenghi, Acton, et al., 1999) and are composed of hemipelagic sediments consisting of an alternation of laminated to thinly bedded orange-brown diatom ooze with blue-gray diatom-bearing terrigenous silt and clays (Fig. F2). These sediments overlie a dense, blue-gray diamict with many prominent dropstones. Overlapping sediment slabs, 15 cm long and ~1 cm wide, were removed from the core using a sediment slab cutter (Pike and Kemp, 1996; Schimmelmann et al., 1990). These slabs were subsampled for thin section preparation and also for examination by SEM secondary electron imagery (SEI).

Sediment for polished thin section preparation was prepared following the fluid-displacive, low-viscosity Spurr resin embedding technique of Pike and Kemp (1996), as adapted by Pearce et al. (1998). Thin sections were analyzed using light microscopy and SEM backscattered electron imagery (BSEI) to document lamina composition and thickness variations and sediment fabric. BSEI analysis was carried out following the standard techniques developed for paleoceanographic analysis of laminated sediments (Grimm, 1992; Kemp, 1990; Pike, 2000). In essence, the BSEI photograph records the differences in the average atomic number and density of the target; therefore, dense terrigenous grains (hence, terrigenous-rich laminations) that have relatively high average atomic numbers and densities produce bright images. Diatom ooze laminae contain diatom frustules that are filled with low-atomic-number, carbon-based resin and therefore produce dark images. In Palmer Deep sediments, the BSEI photomosaic can be considered as a porosity map with dark layers representing highly porous diatom ooze and bright layers representing dense, diatom-bearing terrigenous silt and clay laminae.

In addition to BSEI, thin sections were examined using light microscopy. In plane-polarized light, the diatom ooze layers produce bright images (optically transparent biogenic silica and resin) and the diatom-bearing silt and clay layers produce darker images. This is the opposite

sense to the BSEI images, so care should be taken when examining the figures in this data report.

Sediment Fracture Surface Analysis

Blocks of sediment with dimensions of <0.5 cm were cut from the slabs and carefully fractured open to reveal surfaces parallel and perpendicular to the laminated sediment fabric. These blocks were correlated with corresponding laminae in the BSEI photomosaics. Care was taken not to touch the fractured surfaces with either scalpel or tweezers. Blocks were mounted onto standard SEM stubs using epoxy glue, left to dry at room temperature for 48 hr, and then gold-coated for topographic SEI analysis. Surfaces were analyzed for composition, fabric, and relationships between components.

RESULTS

Laminated Sediment Fabric

Visual examination of the sediment core sections from Core 178-1098A-6H reveals that the thickness of the orange-brown and blue-gray laminae decreases upcore from interval 178-1098A-6H-3, 43 cm, through 6H-1, 0 cm. Laminations range in thickness from 1 mm to 3 cm in Section 178-1098A-6H-1, and from 2 to 3 cm in interval 178-1098A-6H-3, 0–29 cm. Between interval 178-1098A-6H-3, 110 cm, and 6H-3, 43 cm, the blue-gray diamict takes on an orangey hue with four identifiable orange-brown laminae (intervals 178-1098A-6H-3, 52–53.5, 67–68, 96–97, and 109–110 cm). Below interval 178-1098A-6H-3, 110 cm, there are no orange-brown laminae and the orangey hue disappears from the sediment. Detailed comparison and correlation of Hole 1098A with Holes 1098B and 1098C (Table T1) reveals that Hole 1098A has an almost complete sample of the postglacial laminated unit, which permits the radiocarbon chronology that was developed for Hole 1098C (Domack et al., 2001) to be used on Hole 1098A.

BSEI analysis concentrated on samples from Section 178-1098A-6H-2, so the large-scale reduction in average lamina thickness from interval 178-1098A-6H-3, 43 cm, through 6H-1, 0 cm, is not detected, but analysis did reveal that the sediment is laminated on two scales. There is a primary alternation between thick laminae of diatom ooze and diatom-bearing terrigenous sediments (Fig. F2) and also a smaller-scale inclusion of thin biogenic sublaminae within the diatom-bearing terrigenous lamination.

Contacts between the two lamina compositional types vary from sharp (Fig. F3A) to gradational (Fig. F3B) to bioturbated (Fig. F3C). Bioturbation is on a subcentimeter scale and is not seen during visual core inspection. Sharp, gradational, and bioturbated transitions of lamination composition over submillimeter distances is clearly seen using both BSEI and optical light microscopy.

Diatom-Ooze Laminae

All of the diatom-ooze laminations (average thickness = 1.02 cm; standard deviation [SD] = 0.84 cm; range = 0.1–3.6 cm; *N* = 124) examined in Core 178-1098A-6H are dominated by *Chaetoceros* Ehrenberg resting spores (CRS) (Fig. F4). BSEI and light microscopy show that the

T1. Splice tie points, Site 1098, p. 17.

F3. Laminations in diatom ooze, p. 11.

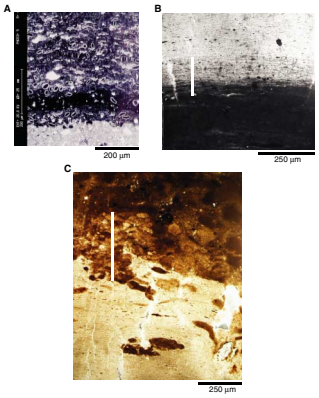

F4. CRS in lamina, p. 13.

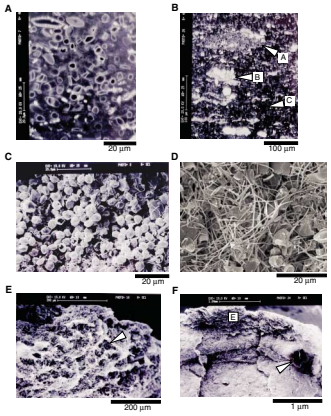

ooze is variable over distances of <100 µm, with areas of densely packed CRS, more porous patches, and silt/clay-rich lenses (Fig. F4B). SEI of horizontal fracture surfaces shows that the CRS-ooze laminae can vary between almost exclusively CRS (Fig. F4C) to CRS with high percentages (up to 50%) of detached setae from the *Chaetoceros* vegetative stages (Fig. F4D). The diatom-ooze laminae also can show a gradation between ooze dominated by CRS and detached setae at the base to pure CRS at the top. SEI of vertical fracture surfaces revealed a very porous fabric characterized by open pore spaces and microtunnels (Fig. F4E). Other diatom taxa are very subordinate to the CRS and are present as isolated valves or as clusters (Fig. F5A).

Thinner diatom-ooze sublaminae (submillimeter) within the thick diatom-bearing terrigenous laminae are dominated by either almost monogeneric assemblage of centric diatoms (Fig. F5C) or, more commonly, *Chaetoceros* setae (Fig. F5E). Centric diatom sublaminae are usually found close to the top of the diatom-bearing terrigenous laminae, including ones produced by *Corethron criophilum* (Fig. F5D). Sublaminae composed of *Chaetoceros* setae are very difficult to detect using BSEI or light microscopy (being only a few microns in thickness); however, fractured surfaces through diatom-bearing terrigenous laminae reveal that setae-rich sublaminae are common (Fig. F5E).

F5. Diatoms in lamina, p. 15.

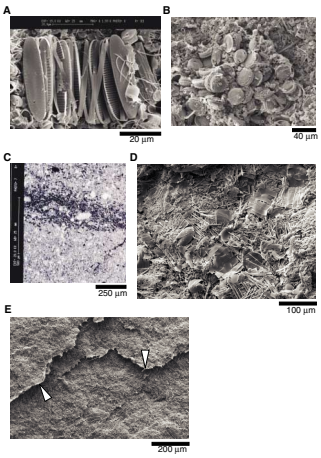

Diatom-Bearing Terrigenous Silt and Clay Laminae

Light microscope analysis of the diatom-bearing terrigenous laminae (average thickness = 1.08 cm; SD = 1.55 cm; range = 0.1–10.4 cm; N = 122) shows that a significant amount of bioturbation affects the fabric (Fig. F3C). SEI analysis of the laminae reveals that the diatom assemblage is much more diverse than within the almost monogeneric ooze. Diatoms are sometimes present as monogeneric clusters within the terrigenous laminae (Fig. F5B). CRS are still common, but the proportion of other centric taxa increases. *Chaetoceros* setae occur throughout the laminae, as well as in discrete sublaminae (Fig. F5E). In general, the frustules within the diatom-bearing terrigenous laminae are less well preserved than frustules in the ooze.

Bioturbation

All methods of analysis used revealed that microbioturbation occurs intermittently through the examined Sections 178-1098A-6H-1 to 6H-3, redistributing material across lamina boundaries (Fig. F3) as well as increasing porosity within the diatom ooze (Fig. F4). The redistribution of sediment occurs over distances of up to 1 cm and, as stated earlier, is not obvious from visual core inspection.

CONCLUSIONS

The regular alternation of diatom ooze with diatom-bearing terrigenous sediment within the postglacial laminated unit from ODP Site 1098, Palmer Deep Basin I, does reflect the modern seasonal variation in flux to the seafloor in the west Antarctic Peninsula region, as influenced by modern oceanographic conditions (Hofmann et al., 1996) and recorded in sediment traps (Leventer, 1991). The detailed microscopic fabric analyses presented here lends support to the hypothesis that this sequence is predominantly composed of annually laminated sediments.

However, our investigations have revealed that there are at least two scales of variation between the diatom ooze and the diatom-bearing terrigenous components—centimeter scale and submillimeter scale. Both scales of variation could be attributed to interannual variability, which would bring the average sedimentation rate of this interval more into line with the AMS radiocarbon-derived sedimentation rate, which would lead to the conclusion that these sediments are not varves. There is also microbioturbation that is not apparent from visual core inspection. Caution should be exercised when using this interval to reconstruct paleoceanographic and paleoclimatic variability during the deglaciation of this region of Antarctica. High-resolution study of the diatom assemblage sequences within both the diatom ooze and diatom-bearing terrigenous laminae, combined with microscale fabric analyses, will clarify whether the sediments are varves or interannual layers.

ACKNOWLEDGMENTS

J.P. would like to acknowledge the receipt of a UK ODP Rapid Response Award and NERC Small Grant GR8/04238, and we thank Franco Ricci Lucchi and Angelo Camerlenghi for their constructive comments, which improved the manuscript. J.P. also would like to thank the participants of the Palmer Deep sampling party at the Bremen ODP Core Repository for helping to compile the detailed correlation between the three holes of ODP Site 1098, shown in Table **T1**, Bob Jones (Southampton Oceanography Centre) for making the polished thin sections, and Jason Hilton for the use of his digital camera.

This research used samples and/or data provided by the Ocean Drilling Program (ODP). ODP is sponsored by the U.S. National Science Foundation (NSF) and participating countries under management of Joint Oceanographic Institutions (JOI), Inc. Funding for this research was provided by the Natural Environment Research Council and the UK Ocean Drilling Program.

REFERENCES

Barker, P.F., Camerlenghi, A., Acton, G.D., et al., 1999. *Proc. ODP, Init. Repts.,* 178 [CD-ROM]. Available from: Ocean Drilling Program, Texas A&M University, College Station, TX 77845-9547, U.S.A.

Blunier, T., Chappellaz, J., Scwander, J., Dällenbach, A., Stauffer, B., Stocker, T.F., Raynaud, D., Jouzel, J., Clausen, H.B., Hammer, C.U., and Johnsen, S.J., 1998. Asynchrony of Antarctic and Greenland climate change during the last glacial period. *Nature,* 394:739–743.

Doake, C.S.M., Corr, H.F.J., Rott, H., Skvarca, P., and Young, N.W., 1998. Breakup and conditions for stability of the northern Larsen Ice Shelf, Antarctica. *Nature,* 391:778–779.

Domack, E., Leventer, A., Dunbar, R., Taylor, F., Brachfeld, S., Sjunneskog, C., and ODP Leg 178 Science Party, 2001. Chronology of the Palmer Deep Site, Antarctic Peninsula: a Holocene paleoenvironmental reference for the circum-Antarctic. *The Holocene,* 11:1–9.

Domack, E.W., Mashiotta, T.A., Burkley, L.A., and Ishman, S.E., 1993. 300-year cyclicity in organic matter preservation in Antarctic fjord sediments. *In* Kennett, J.P. and Warnke, D.A. (Eds.), *The Antarctic Paleoenvironment: A Perspective on Global Change, Part 2*. Antarct. Res. Ser., 60:265–272.

Domack, E.W., and McClennen, C.E., 1996. Accumulation of glacial marine sediments in fjords of the Antarctic Peninsula and their use as late Holocene paleoenvironmental indicators. *In* Ross, R.M, Hofmann, E.E., Quentin, L.B. (Eds.), *Foundations for Ecological Research West of the Antarctic Peninsula*. Antarct. Res. Ser., 70:135–154.

Grimm, K.A., 1992. High-resolution imaging of laminated biosiliceous sediments and their paleoceanographic significance (Quaternary, Site 798, Oki Ridge, Japan Sea). *In* Pisciotto, K.A., Ingle, J.C., Jr., von Breymann, M.T., Barron, J., et al., *Proc. ODP, Sci. Results,* 127/128 (Pt. 1): College Station, TX (Ocean Drilling Program), 547–557.

Hofmann, E.E., Klinck, J.M., Lascara, C.M., and Smith, D.A., 1996. Water mass distribution and circulation west of the Antarctic Peninsula and Bransfield Strait. *In* Ross, R.M, Hofmann, E.E., Quentin, L.B. (Eds.), *Foundations for Ecological Research West of the Antarctic Peninsula*. Antarct. Res. Ser., 70:61–80.

Jones, P.D., Marsh, R., Wigley, T.M.L., and Peel, D.A., 1993. Decadal timescale links between Antarctic Peninsula ice-core oxygen-18, deuterium and temperature. *The Holocene,* 3:14–26.

Kemp, A.E.S., 1990. Sedimentary fabrics and variation in lamination style in Peru continental margin upwelling sediments. *In* Suess, E., von Huene, R., et al., *Proc. ODP, Sci. Results,* 112: College Station, TX (Ocean Drilling Program), 43–58.

Leventer, A., 1991. Sediment trap diatom assemblages from the northern Antarctic Peninsula region. *Deep-Sea Res.,* 8/9:1127–1143.

Leventer, A., Domack, E.W., Ishman, E., Brachfeld, S., McClennen, C.E., and Manley, P., 1996. Productivity cycles of 200–300 years in the Antarctic Peninsula region: understanding linkages among the sun, atmosphere, oceans, sea ice, and biota. *Geol. Soc. Am. Bull.,* 108:1626–1644.

Leventer, A., Dunbar, R.B., and DeMaster, D.J., 1993. Diatom evidence for late Holocene climatic events in Granite Harbor, Antarctica. *Paleoceanography,* 8:373–386.

Leventer, A., Pike, J., Domack, E., Taylor, F., Sjunneskog, C., Dunbar, R., McAndrews, E., and ODP Leg 178 Scientific Party, 1998. Varves from the Palmer Deep. *EOS, Trans., AGU,* 79 (Supplement):F518.

Morris, K., Jeffries, M.O., and Li, S., 1998. Sea ice characteristics and seasonal variability of ERS-1 SAR backscatter in the Bellingshausen Sea. *In* Jeffries, M.O. (Ed.), *Ant-*

arctic Sea Ice: Physical Processes, Interactions and Variability. Washington, D.C. (Am. Geophys. Union), 213–242.

Parkinson, C.L., 1998. Length of the sea ice season in the Southern Ocean, 1988–1994. *In* Jeffries, M.O. (Ed.), *Antarctic Sea Ice: Physical Properties, Interactions and Variability.* Washington, D.C. (Am. Geophys. Union), 173–186.

Pearce, R.B., Kemp, A.E.S., Koizumi, I., Pike, J., Cramp, A., and Rowland, S.J., 1998. A lamina-scale, SEM-based study of a late Quaternary diatom-ooze sapropel from the Mediterranean Ridge, Site 971. *In* Robertson, A.H.F., Emeis, K.-C., Richter, C., and Camerlenghi, A. (Eds.), *Proc. ODP, Sci. Results,* 160: College Station, TX (Ocean Drilling Program), 349–363.

Pike, J., 2000. *Data report:* Backscattered electron imagery analysis of early Pliocene laminated *Ethmodiscus* ooze, Site 1010. *In* Lyle, M., Koizumi, I., Richter, C., and Moore, T.C. (Eds.), *Proc. ODP, Sci. Results,* 167: College Station, TX (Ocean Drilling Program), 207–212.

Pike, J., and Kemp, A.E.S., 1996. Preparation and analysis techniques for studies of laminated sediments. *Spec. Publ.—Geol. Soc. London,* 116:37–48.

Pudsey, C.J., Barker, P.F., and Larter, R.D., 1994. Ice sheet retreat from the Antarctic Peninsula shelf. *Cont. Shelf Res.,* 14:1647–1675.

Rebesco, M., Camerlenghi, A., DeSantis, L., Domack, E.W., and Kirby, M.E., 1998. Seismic stratigraphy of Palmer Deep: a fault-bounded Late Quaternary sediment trap on the inner continental shelf, Antarctic Peninsula Pacific margin. *Mar. Geol.,* 151:89–110.

Schimmelmann, A., Lange, C.B., and Berger, W.H., 1990. Climatically controlled marker layers in Santa Barbara basin sediments, and fine-scale core-to-core correlation. *Limnol. Oceanogr.,* 35:165–173.

Smith, D.A., Hofmann, E.E., Klinck, J.M., and Lascara, C.M., 1999. Hydrography and circulation of the West Antarctic Peninsula Continental Shelf. *Deep-Sea Res. I,* 46:925–949.

Figure F1. Location of Palmer Deep, west Antarctic Peninsula (Barker, Camerlenghi, Acton, et al., 1999).

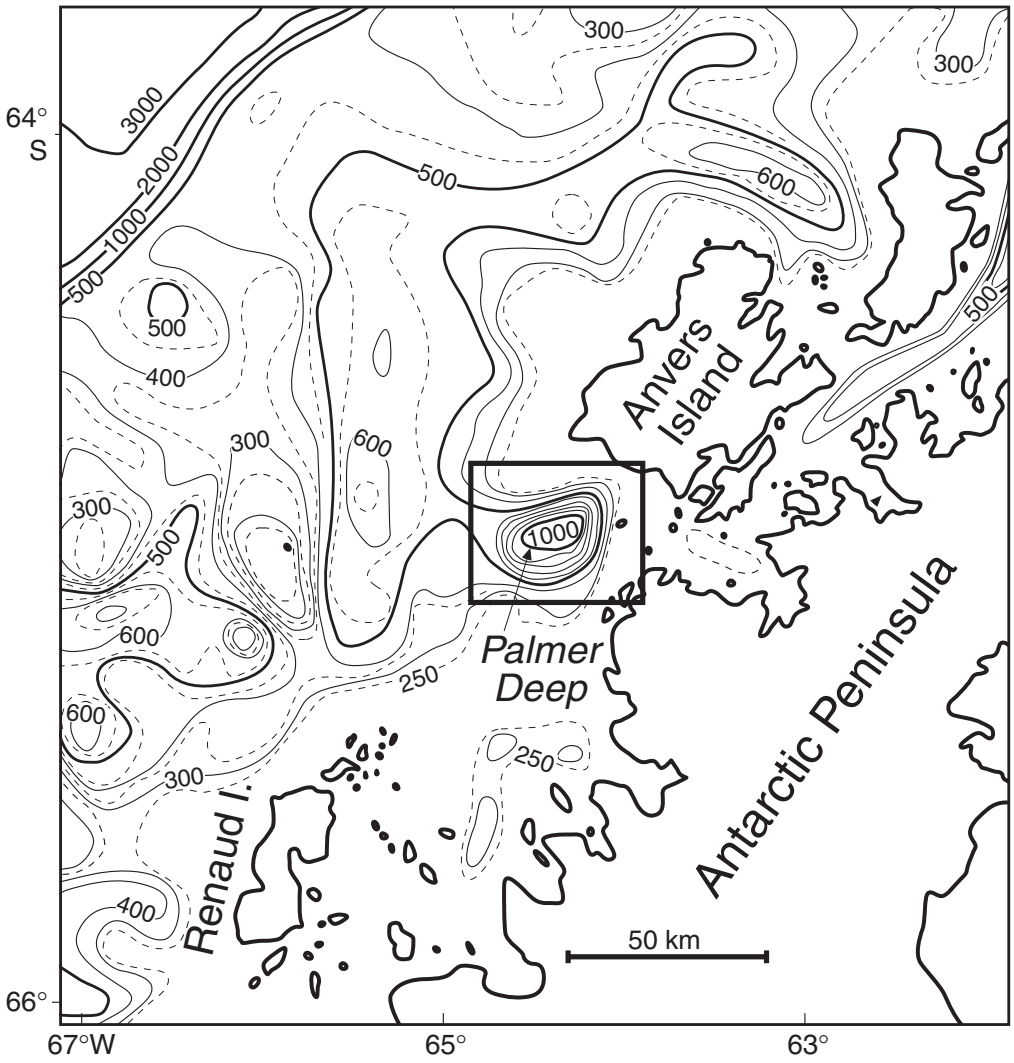

Figure F2. Core photograph of Core 178-1098A-6H. Darker laminae are composed of orange-brown diatom ooze, and lighter laminae are composed of blue-gray diatom-bearing terrigenous silt and clays. Prominent dropstones in interval 178-1098A-6H-3, 65–75 cm, mark the boundary between the postglacial, hemipelagic "laminated unit" above and the glacial to early postglacial diamict below.

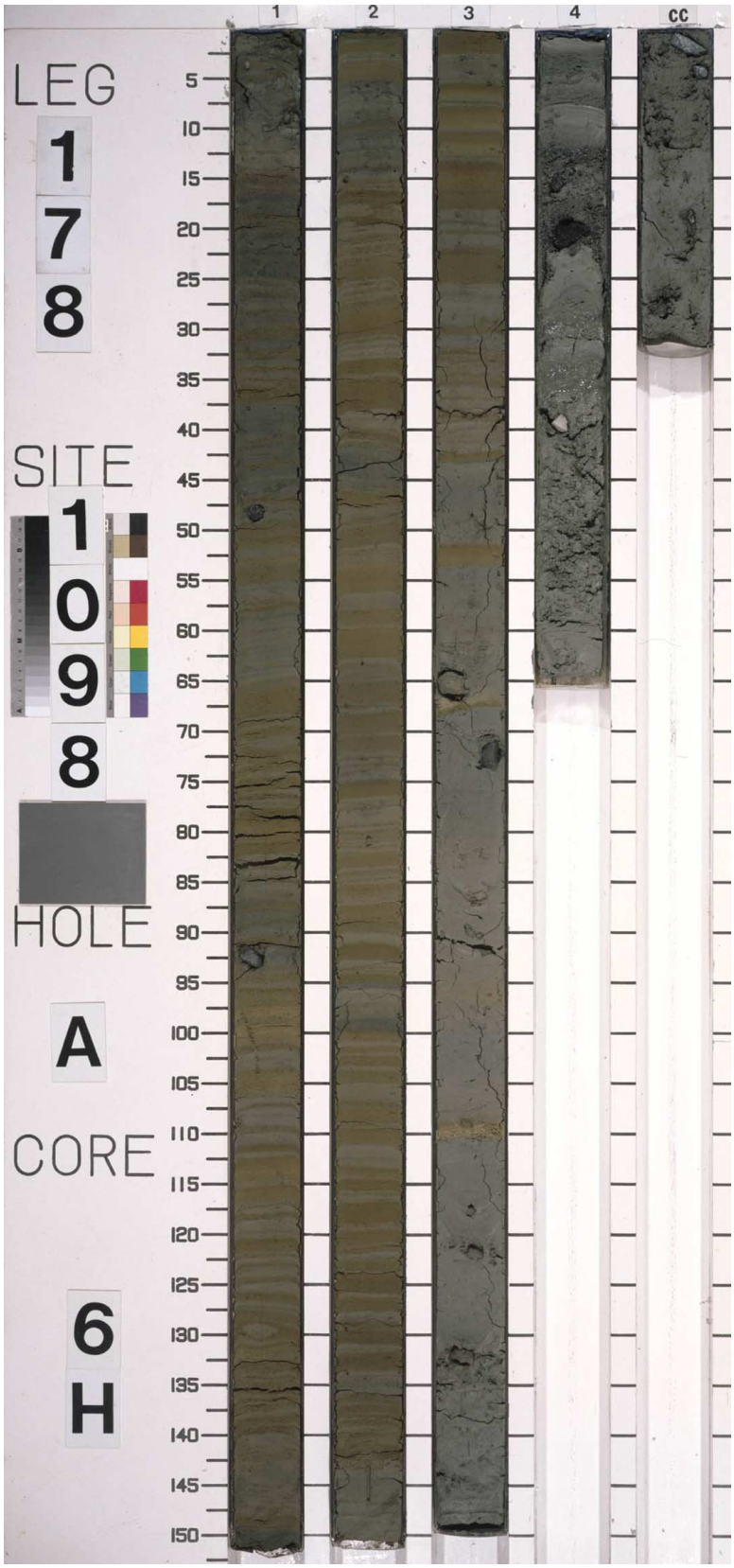

Figure F3. A. BSEI micrograph showing bright, high-backscatter coefficient diatom-bearing terrigenous silt and clays overlain by darker, low-backscatter coefficient diatom ooze. Contact between laminations is very sharp (Sample 178-1098A-6H-3, 4.5–8 cm). **B.** Light microscope micrograph of opaque, diatom-bearing terrigenous lamina composed of silts and clays overlain by transparent diatom-ooze lamina. Contact between the two laminations is gradational over the region indicated by the white vertical line (Sample 178-1098A-6H-2, 127.3–131.6 cm). **C.** Light microscope micrograph showing transparent diatom-ooze lamina overlain by opaque diatom-bearing terrigenous silt and clays. Contact between the two laminations is bioturbated. Mixing of sediment at the boundary occurs across the distance marked by the vertical white line. Dark patches within the diatom ooze in the lower half of the micrograph are cross sections through deeper burrows where diatom-bearing terrigenous material has been taken down through the sediment. The mottled appearance of the upper, diatom-bearing terrigenous lamination is characteristic of bioturbation (Sample 178-1098A-6H-3, 50–54.5 cm). (**Figure shown on next page.**)

Figure F3 (continued). (Caption shown on previous page.)

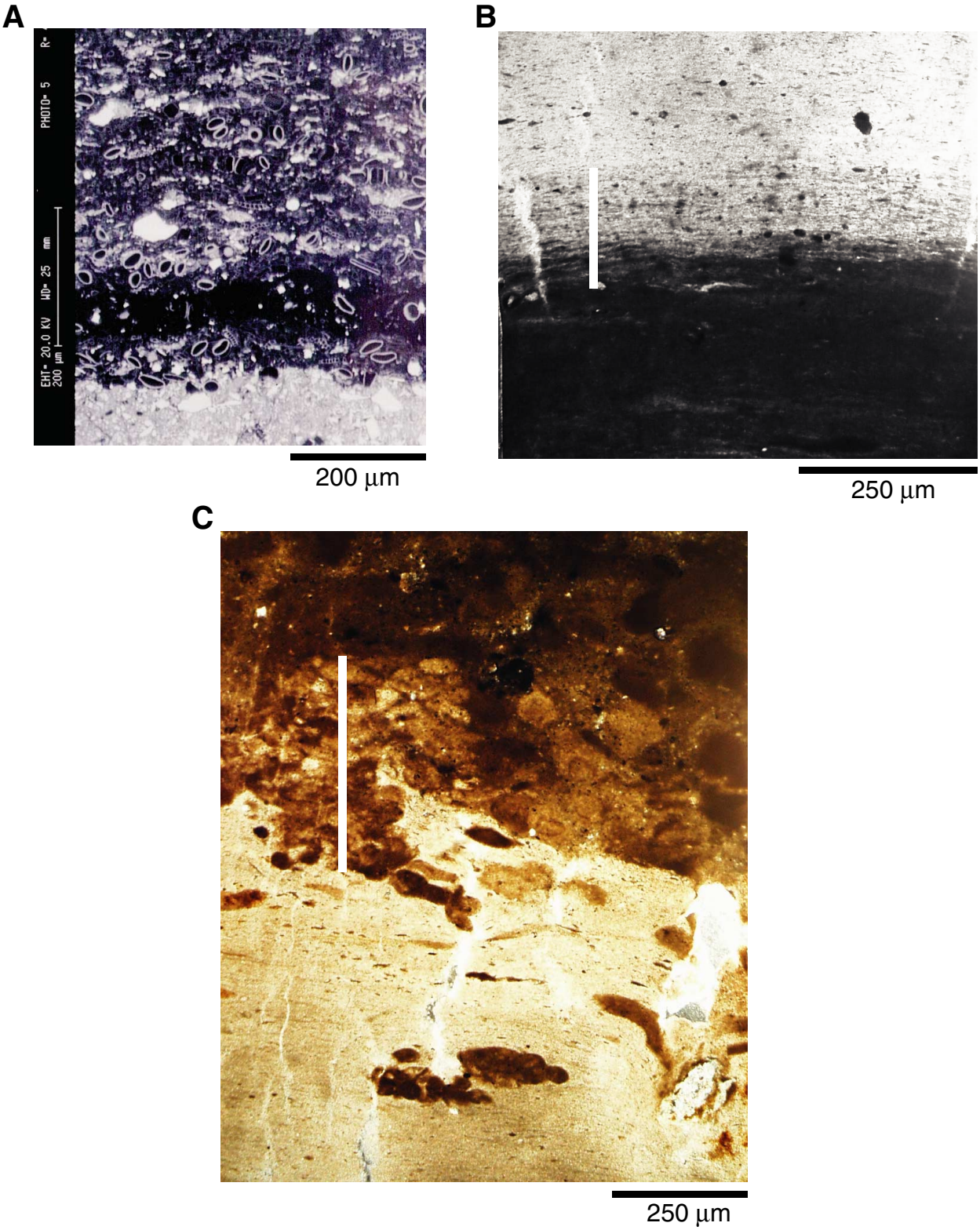

Figure F4. A. BSEI micrograph showing *Chaetoceros* resting spore-dominated diatom-ooze lamina (Sample 178-1098A-6H-1, 144 cm). **B.** BSEI micrograph showing the variation of fabric within the diatom-ooze laminae. A = closely packed *Chaetoceros* resting spores, possible remnants of fecal pellet; B = closely packed terrigenous aggregate, again possible remnants of fecal pellet; C = area of higher porosity, a result of burrows being preserved within the diatom ooze structure (see part E below) (Sample 178-1098A-6H-3, 4.5–8.5 cm). **C.** SEI micrograph of fractured lamina-parallel surface through diatom ooze. Ooze is comprised almost exclusively of *Chaetoceros* resting spores with few detached setae (Sample 178-1098A-6H-1, 54.1 cm). **D.** SEI micrograph of lamina-parallel fracture surface through diatom ooze. Ooze is comprised of *Chaetoceros* resting spores and ~50% detached setae from the vegetative stage of the *Chaetoceros*. Both C and D demonstrate the gradation within diatom-ooze laminae from CRS ooze dominated by detached setae in the lower parts to CRS ooze with very few detached setae in the higher parts (Sample 178-1098A-6H-1, 54.4 cm). **E.** SEI micrograph of vertical fracture surface through a diatom-ooze lamina. Microtunnels and pores are indicated by arrows. These are interpreted as remnant burrow structures (Sample 178-1098A-6H-3, 54–54.3 cm). **F.** SEI micrograph of vertical fracture surface from a diatom-bearing terrigenous lamina up into a diatom ooze lamina through a bioturbated contact. A large tubelike burrow runs along the contact, one end of which is indicated by an arrow. E = the position of E, above. Below the burrow, you can see the frayed edges of setae sublaminae within the diatom-bearing terrigenous lamina (also see Fig. **F5E,** p. 15) (Sample 178-1098A-6H-3, 54–54.3 cm). (**Figure shown on next page.**)

Figure F4 (continued). (Caption shown on previous page.)

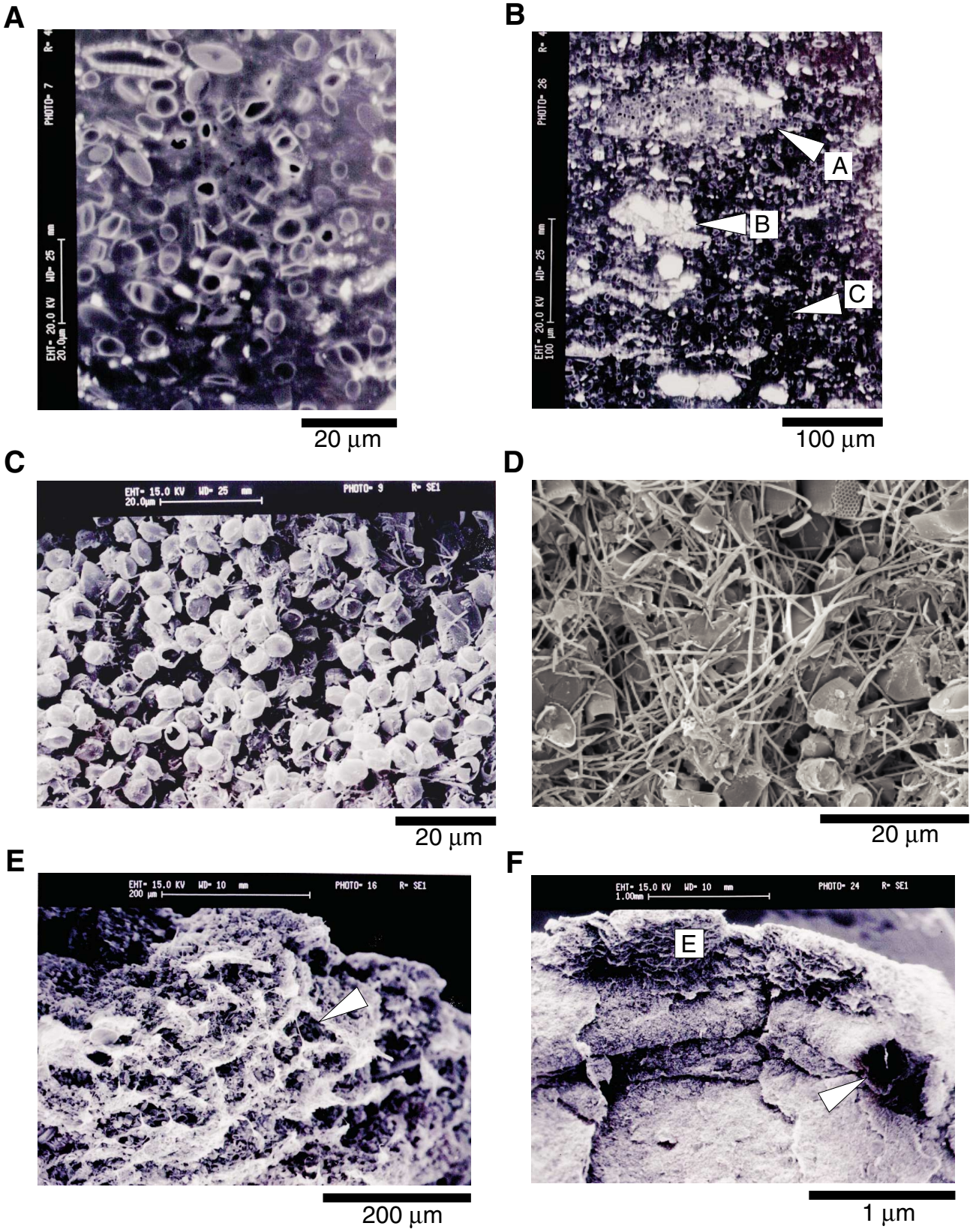

Figure F5. A. SEI micrograph of a cluster, or intact colony, of *Fragilariopsis* pennate diatoms within a diatom-ooze lamina (Sample 178-1098A-6H-1, 54.1 cm). **B.** SEI micrograph of a cluster of *Thalassiosira antarctica* within the very top of a diatom-bearing terrigenous lamina, possibly a remnant of a fecal pellet (Sample 178-1098A-6H-1, 52.1 cm). **C.** BSEI micrograph through a centric diatom sublamina within a diatom-bearing terrigenous lamina. The darker, lower backscatter coefficient diatom sublamina is ~250 µm thick (Sample 178-1098A-6H-3, 4.5–8 cm). **D.** SEI micrograph of *Corethron criophilum* sublamina from the mid-to-base region of a diatom-bearing terrigenous lamina (Sample 178-1098A-6H-1, 53.8 cm). **E.** SEI micrograph of a lamina-parallel fracture surface through a diatom-bearing terrigenous lamina. Frayed edges of *Chaetoceros* setae sublaminae are indicated by arrows (Sample 178-1098A-6H-1, 53.6 cm). (**Figure shown on next page.**)

Figure F5 (continued). (Caption shown on previous page.)

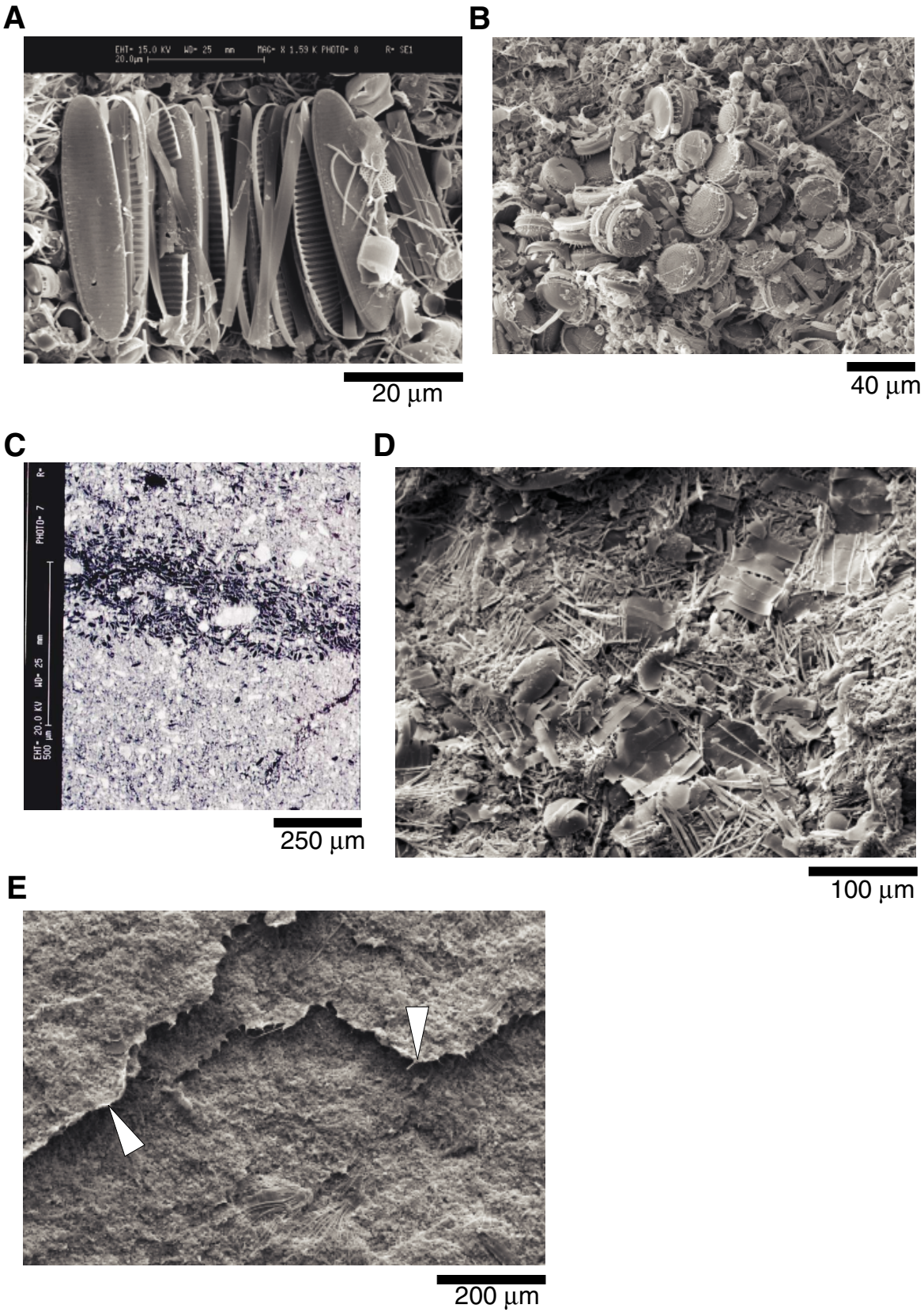

Table T1. Correlation of the postglacial laminated unit between Holes 1098A, 1098B, and 1098C as constructed at the Palmer Deep Sites Sampling Party, ODP Core Repository, Bremen.

Core, section, interval (cm)		Core, section, interval (cm)		Core, section, interval (cm)
178-1098A-		178-1098B-		178-1098C-
		5H-5, 119	Ties to	5H-2, 39.5*
		5H-5, 138	Ties to	5H-2, 58*
6H-1, 14.5	Ties to			5H-2, 115
6H-1, 29.5	Ties to	5H-6, 15.5		
6H-1, 41	Ties to	5H-6, 23		
6H-1, 55	Ties to	5H-6, 31	Ties to	5H-3, 6.5
6H-1, 66.5	Ties to	5H-6, 43		
		5H-6, 68	Ties to	5H-3, 41
		5H-6, 81	Ties to	5H-3, 52.5
6H-1, 122	Ties to	5H-6, 98		
6H-2, 1.5	Ties to	1H-6, 121		
6H-2, 38	Ties to	5H-7, 3.5		

Note: * = slumped sediment.